

NASA CR-174,606

NASA-CR-174606
19840005480

A Reproduced Copy OF

NASA CR-174,606

*High Energy Efficient
Solid State Laser Sources*

R.L. Byer

Reproduced for NASA

by the

NASA Scientific and Technical Information Facility

LIBRARY COPY

1984

LANGLEY RESEARCH CENTER
LIBRARY, NASA
HAMPTON, VIRGINIA

FFNo 672 Aug 65



NF00416

DRA

HIGH ENERGY EFFICIENT SOLID STATE LASER SOURCES



Annual Technical Report
covering the period
June 1, 1982 - May 31, 1983

(NASA-CR-174606) HIGH ENERGY EFFICIENT
SOLID STATE LASER SOURCES Annual Technical
Report, 1 Jun. - 31 May 1983 (Stanford
Univ.) 45 p HC A03/MF A01 CSCI 20E

N84-13548

Unclass
G3/36 15233

NASA Grant NAG 1-182

Robert L. Byer
Principal Investigator

G.L. Report No. 3634
October 1983

Edward L. Ginzton Laboratory
W.W. Hansen Laboratories of Physics
Stanford University
Stanford, CA 94305

AW

N84-13548

HIGH ENERGY EFFICIENT SOLID STATE LASER SOURCES

Robert L. Byer
Applied Physics Department
Stanford University
Stanford, California 94305

ABSTRACT

During the second year of this program we have extended our slab glass performance studies and have demonstrated 18 J of output at 2 Hz with 2.3% wall plug efficiency. Our goal is to achieve 10 J per pulse at 10 Hz and 3% wall plug efficiency during the next annual period.

We have extended the slab concept to Nd:YAG and to Nd:GGG. To date over 30 W of cw output power at 2% efficiency has been generated in slab Nd:YAG. We have invented a multi-plexed slab Nd:YAG pre-amplifier and plan to verify its performance during the next program period. We have demonstrated a Nd:YAG oscillator with 100 kHz linewidth for eventual use in wind velocity measurements.

TABLE OF CONTENTS

	<u>Page</u>
ABSTRACT.....	iii
TABLE OF CONTENTS.....	iii
I. INTRODUCTION.....	1
A. Progress in Slab Geometry Laser Sources.....	1
B. Single Frequency Nd:YAG for Remote Wind Measurements.	1
II. SUMMARY OF RESEARCH PROGRESS.....	2
A. Slab Geometry Nd:Glass Laser Research.....	2
B. Slab Geometry Nd:YAG Laser Research.....	5
1. Slab geometry Nd:YAG studies.....	5
2. Design and fabrication of a multiplexed slab amplifier.....	7
3. Design of diode laser pumped single frequency Nd:YAG local oscillator.....	8
4. Design studies for diode array pumped Nd:YAG slab geometry lasers.....	9
C. Solid State Tunable Sources.....	10
III. CONCLUSION.....	12
IV. REFERENCES.....	14
V. PUBLICATIONS AND PRESENTATIONS.....	15

Table of Contents - cont.

	Page
APPENDICES.....	16
APPENDIX A:	17
Sub-megahertz Frequency Stabilized Nd:YAG Oscillator.	
APPENDIX B:	20
Solid State Lasers for Remote Sensing.	
APPENDIX C:	27
Reduced Thermal Focusing and Birefringence in Zig-Zag Slab Geometry Crystalline Lasers.	

HIGH ENERGY EFFICIENT SOLID STATE LASER SOURCES

Robert L. Byer

I. INTRODUCTION

A. Progress in Slab Geometry Laser Sources

During the past year we have made rapid progress in slab glass and slab Nd:YAG laser source development. We have achieved operation of high doped Nd:Glass with 18J output at 2Hz with 2.3% wall plug efficiency in long pulse mode operation.^{1,2} We expect to generate up to 15J at 5Hz with 2.5% efficiency by the end of this program period.

Our conduction cooling approach³ has enabled us to design high average power slab glass laser sources. Recent design improvements using transverse oriented flashlamps should lead to improved pumping uniformity and efficiency.

To date we have generated 80W at 2% efficiency from slab Nd:YAG.⁴ With new power supplies we expect to demonstrate over 200W of average power at 2% efficiency.

Our research has led to a better understanding of slab geometry laser design. In addition, we have identified the amplification of low power narrow linewidth Nd:YAG as the key technical issue in proposed wind measurements. We have invented a multiplexed slab amplifier to achieve the amplification in a very efficient manner.⁵

B. Single Frequency Nd:YAG for Remote Wind Measurements

During the past year we demonstrated single axial mode operation of Nd:YAG with 100 kHz linewidth.⁶ We propose to extend our studies to diode laser pumped Nd:YAG as a very narrow linewidth cw local oscillator source.

This diode pumped local oscillator will be followed by the spatially multiplexed Nd:YAG slab amplifier to provide the output energy required for remote sensing of wind.

II. SUMMARY OF RESEARCH PROGRESS

A. Slab Geometry Nd:Glass Laser Research

Our work on slab Nd:Glass development is outlined in Table I. Previously, we have demonstrated the ability to tune the Nd:Glass laser and the ability to frequency shift the Nd:Glass laser by harmonic generation and by stimulated Raman processes. Our recent work, therefore, has concentrated on methods of improving the Nd:Glass slab performance. Table I outlines the progress we have made along this line.

Our initial work to demonstrate the slab laser performance was conducted in a test-bed laser constructed in 1981. The test-bed laser has allowed us to operate at up to 10 joules of output energy at $2\frac{1}{2}$ Hz repetition rate with 1.6% efficiency. The test-bed laser was succeeded by a laser using higher doped phosphate glass which has operated at up to 18 joules per pulse at 2 Hz repetition rate or 36 watts of average power. An important feature of the second generation slab laser is its use of helium gas as the coolant in place of fluids.

We have proceeded to extend the research of the helium conduction cooled slab glass laser in our current Nd:Glass slab which uses a slab 30 centimeters long by 4.5 centimeters wide by .65 centimeters thick of 8% doped phosphate Nd:Glass. This laser, which is called the 'SAVIC' laser is our current slab laser device for research studies. The SAVIC laser has, to date, operated at 15 joules per pulse at 5 Hz repetition rate or 75 watts of average power at an efficiency of 1.5%. We have pumped the SAVIC laser with both longitudinal flashlamps and recently with transverse flashlamps.

TABLE I

Slab Laser Demonstrated and Projected Performance
Stanford University

Nd:Glass

<u>Date</u>	<u>Laser System</u>	<u>Performance</u>
October 1981	15cm x 2.5cm x .83cm 3% doped phosphate glass fluid cooled test-bed laser	10J 2.5Hz 1% efficiency 25W average power
October 1982	15cm x 2.5cm x .65cm 8% doped phosphate glass helium conduction cooled	18J 2Hz 2.3% efficiency 36W average power
June 1983	30cm x 4cm x .65cm 8% doped phosphate glass helium conduction cooled longitudinal flashlamps	15J 5Hz 1.5% efficiency 75W average power
December 1983	30cm x 4cm x .65cm 8% doped phosphate glass helium conduction cooled transverse flashlamps	10J 10Hz 3% efficiency 100W average power



Table I cont.

<u>Date</u>	<u>Laser System</u>	<u>Performance</u>
August 1982	10cm x .8cm x .4cm Nd:YAG cw lamp pumped (4kW)	80W cw 2% efficiency
November 1983	10cm x .8cm x .4cm Nd:YAG cw lamp pumped (10kW)	200W cw 2% efficiency
December 1983	10cm x .8cm x .4cm Nd:YAG multiplexed slab amplifier	30mJ at 20Hz TEM ₀₀ mode, single axial mode

We prefer to pump the SAAVIC laser with transverse flashlamps because of the more uniform pumping achieved and because of the lower voltage required to drive the system. We plan to operate the SAAVIC laser as an oscillator/amplifier later in the year. The design goal for that system is a Nd:Glass laser with a 10 joule per pulse energy operating at 10 Hz repetition rate or 100 watts average power.

The SAAVIC Nd:Glass slab laser is also useful for amplifying Nd:YAG laser radiation. We plan, during the coming year, to test the performance of the Nd:slab amplifier with a Nd:YAG input source. Our design calculations show that it is possible to generate up to 6 joules per pulse at 10 Hz repetition rate using the SAAVIC as an amplifier following the Nd:YAG laser source. Questions that need to be answered in this YAG:Glass oscillator/amplifier combination are the gain at 1.064 micrometers in the neodimium phosphate glass and concern for superfluorescence gain limitations in the slab amplifier.

In summary, progress that we have made during the last year in the slab glass program include the engineering and the design of the slab glass laser head, the purchase and operation of the 20 kilowatt power supplies required to drive the laser source, the invention and demonstration of helium gas conduction cooling in the slab laser, engineering and finally the operation of the glass laser to the performance levels listed in Table I.

B. Slab Geometry Nd:YAG Laser Research

1. Slab geometry Nd:YAG studies. Table I also summarizes the progress we have made in applying the slab geometry concept to the Nd:YAG laser. Our first Nd:YAG slab laser was constructed using a conventional, commercial cw Nd:YAG housing. That laser demonstrated output power of 80 watts cw at 2% efficiency. The threshold and efficiency were very nearly the same for the

as the rod for which the slab substituted. However, the thermal distortion was significantly less for the slab than for the rod. The thermal focusing was 1/6th as strong as for the slab as for the rod and the thermal depolarization was less than 1% of that for the rod. We have submitted a letter to the I.E.E.E. Journal of Quantum Electronics describing this work, (see Appendix III).

The Nd:YAG slab lasers that have been built so far have had a rectangular cross-section with a width twice their thickness. This is necessary to avoid distortion near the slab edges which is not cancelled by simply using the slab geometry. We have shown theoretically that this distortion can be completely eliminated if the laser polarization, the angle of propagation through the slab and the orientation of the crystal axis are chosen correctly. This would make possible slabs of square cross-section with the same advantages as the current rectangular slabs. However, it would save considerably in the Nd:YAG material costs and also give better pumping efficiency for TEM₀₀ mode operation. We plan to carry out experiments to verify the theory in the coming year.

We have also calculated the dependence of the transmitted wave flatness on the optical figure of the slab surfaces. This makes it possible for us to calculate the fabrication tolerances required for slab lasers. The most critical tolerance is the flatness of the total reflection surface in the direction perpendicular to the propagation direction of the beam. Early slabs had significant focusing power at zero input pump power because of the fabrication tolerances. We now have the capability of fabricating slab YAG lasers within the flatness tolerances required.

During the past year we have applied a computer model of the slab geometry laser to predict the thermal effects of the slab crystalline laser. The model allows us to predict the effects of orientation with respect to the crystalline axis of slab medium. The relationship between stress and changes in the index of refraction through the elasto-optic tensor for Nd:YAG is highly anisotropic so the choice of crystalline orientation is quite significant. To minimize de-polarization it is desirable to have the 112 axis of the crystal perpendicular to the plane of the zig-zag path. At fairly high pump powers the de-polarization in the wrong orientation can exceed that of the correct orientation by a factor of 3 according to our computer model. We have also derived crystalline orientation conditions for the propagation without de-polarization through a zig-zag slab made of uniaxial or biaxial crystalline material. The condition is that one of the eigenvectors of the dielectric tensor must be perpendicular to the plane of the zig-zag path. We propose to initiate an experimental verification of the slab orientation using Nd:YLF material since the output of the Nd:YLF crystal matches that of the Nd:Glass amplifier that could be used for more efficient output energy.

2. Design and fabrication of a multiplexed slab amplifier. The remote wind velocity measurement system which is envisioned will consist of a stable cw oscillator operating at about 0.1 watt. The transmitted pulses will be 1 microsecond, 100 kilowatt pulses. Thus an amplifier gain of one million is needed. Flash pumped Nd:YAG amplifiers can have gains as high as 100 per pass. Thus we need a minimum of three passes. The slab geometry creates the opportunity for many passes through the same piece of material while easily separating the beams outside the slab. Paths through the slab with different numbers of total internal reflections propagate at different

angles outside the slab, for simple geometric reasons. Thus a slab laser head accessible from many angles is desirable. We have designed and are building such a laser head.

3. Design of diode laser pumped single frequency Nd:YAG local oscillator.

The key component of our wind velocity measuring system is a single mode, frequency stable Nd:YAG laser. We built a flash pumped quasi-cw version which showed stability of about 100 kilohertz for 5 msec which is more than adequate remote wind velocity measurements for a time delay corresponding to a 800 km altitude of an orbiting satellite.⁶ (See Appendix I). We used this laser to measure the speed of a spinning wheel in the laboratory by observing the Doppler shift of the light reflected from a rotating wheel. The reflected light was interfered with a beam delayed 6 microseconds by passage through an optical fiber. Accurate measurements were possible, demonstrating the stability of the laser at least for the moderate time delay involved. Note that the 100 kHz frequency stability corresponds to a wind velocity of 10 cm/sec at 1.06 μm .

Recently we have extended the concept of the cw local Nd:YAG oscillator to a cw dye laser pumped YAG oscillator. In this case we used an argon pumped dye laser as a replacement for a small diode laser. The dye laser pumped Nd:YAG oscillator consists of a 6 millimeter long YAG crystal, 2 millimeters in diameter. This small YAG crystal is co-axially pumped by the dye laser. It has an optical resonator fabricated on the end of the YAG crystal which is coated with dielectric coatings. We have demonstrated that this small monolithic YAG oscillator has a threshold pump power of 15 milliwatts and has operated at an output power up to 8 milliwatts single axial mode. Recently we have constructed two NdYAG oscillators, pumped by

the same dye laser source. Optical beat experiments between these independent YAG oscillators has shown that they have a free running linewidth of 200 kilohertz in a 1 second integration period. The instantaneous linewidth of these YAG oscillators has been shown to be on the order of 2 kilohertz. The experiment was very preliminary in that the Nd:YAG oscillators were mounted on an open table and no care was taken to isolate them from the acoustic environment.

We are now designing a small diode pumped laser. It will be strictly cw, thus eliminating problems with transients and with chirp caused by the heating of the laser rod. The diode pumping results in a minimum of waste heat, allowing for conduction cooling and elimination of vibrations caused by the water coolant. The output from the diode is also more stable than the lamp it replaces. For all these reasons, diode pumping is desirable.

The diode pumped Nd:YAG laser will make use of a number of novel design features. The entire resonator will consist of one crystal with the mirrors being the facets of the crystals. Thus resonator instability due to mirror motion will be greatly reduced. Single mode operation will be insured by building the laser as a ring laser, with a permanent magnetic field creating a preferred direction for lasing. The ring laser also provides isolation against light reflected back into the laser, a critical factor when designing for stability in operation. Excellent open loop frequency stability is expected. We have obtained a 50 mW diode laser from Xerox for these experiments.

4. Design studies for diode array pumped Nd:YAG slab geometry lasers.

The use of laser transmitters for remote sensing from high altitude aircraft or from space platforms places strict design rules on the laser source. For free-flying satellite based LIDAR, the laser transmitter must operate at greater than 2-5% overall efficiency for lifetimes approaching 3-5 years.

These goals can be met by an all solid state laser transmitter. We propose to carry out preliminary system design calculations for a GaAs diode array pumped slab geometry Nd:YAG laser source. The goal of the study is to derive design rules to aid in predicting diode array pumped Nd:YAG performance characteristics. Experimental studies of diode array pumped Nd:YAG concept should be possible in our laboratory using diode arrays supplied by the Xerox Palo Alto Research Center. Our preliminary analysis has shown that diode array pumped Nd:YAG is capable of operating at efficiencies as high as 15%. The principle technical risk is the design construction and cooling of the diode arrays used for pumping the Nd:YAG source.

C. Solid State Tunable Sources

The two classes of solid state tunable sources are laser based devices and parametric based devices. Examples of the former include F-center lasers,⁷ transition metal ion lasers^{8,9} and doped oxide and fluoride crystalline lasers. Examples of the later include Nd:YAG pumped LiNbO₃ parametric oscillator^{10,11} and the recently demonstrated AgGaS₂ parametric oscillator¹² with a potential tuning range from 1.3 - 12 μm in the infrared.

The F-center laser devices have the potential to tune over the near infrared region from .8 μm to beyond 3 μm . However, cryogenic operation is required. Furthermore, each crystal tunes over a narrow region limited by the gain bandwidth product of the laser transition.⁷

An alternative to the F-center laser is the transition metal ion laser such as Ni⁺⁺MgF₂ and Co⁺⁺MgF₂ developed by Moulton of Lincoln Laboratories.⁸ These devices are laser pumped and tune over the 1.6 - 2.1 μm range. They also require cryogenic cooling. The low gain cross-section of the phonon assisted

transition metal ion lasers leads to oscillator operation in TEM₀₀ mode and to low pulse energy output. The low gain also prevents amplifier operation to increase the output level.

Frequency extension of the Co⁺⁺MgF₂ laser is possible by harmonic generation in LiNbO₃ and by parametric oscillation in AgGaSe₂. We plan to cooperate with Peter Moulton in the application of AgGaSe₂ to infrared generation by OPO using the Co⁺⁺MgF₂ pump laser.

Recent work by Huber in Germany has identified Cr⁺⁺⁺:GScGG as a tunable source in the .7 - .8 μm region.¹³ This tunable Garnet crystal host laser is similar to the Alexandrite laser introduced by Walling.⁸ However, the Garnet host material offers flexibility in the crystal parameters and ease of growth not available in Alexandrite. The tuning range of the GdScCaG laser extends from .7 - .8 μm. The laser operates at room temperature and can be flashlamp pumped or laser pumped by the second harmonic of Nd:YAG.

The Cr⁺⁺⁺ doped oxide crystals offer a new approach to an all solid state tunable source. The primary tuning range can be extended by harmonic generation and by mixing toward both the ultraviolet and the infrared.

Three groups in the United States are now studying the Garnet crystals. Crystals are being grown under support by Lincoln Laboratory and Lawrence Livermore National Laboratory. We expect sample crystals to be available soon for optical pumping studies.

Recently Ti⁺⁺⁺Al₂O₃ was introduced by Moulton as a d-level laser transition that is also tunable in the .73 - .83 μm range.¹⁴ This laser offers the possibility of tunable output again by laser pumping at the second harmonic of Nd:YAG. At Stanford we have initiated growth studies of Ti⁺⁺⁺Al₂O₃ using our fiber growth apparatus. Our goal is to study the potential for tunable output from this new oxide based tunable source.

The above tunable sources offer tuning capability over a 1500 cm^{-1} tuning range in the near infrared. Frequency extension by harmonic generation and by mixing is possible using well developed nonlinear crystals such as KDP and LiNbO_3 . For example, LiNbO_3 allows extension to $4 \text{ }\mu\text{m}$ in the infrared.

Future frequency extension in AgGaS_2 is possible to $12 \text{ }\mu\text{m}$. This chalcopyrite crystal is being grown at Stanford University under partial support by N.A.S.A.

Thus an all solid state tunable source is possible to design using well known Nd:YAG technology as the primary pump laser. Frequency extension involves the use of new tunable solid state laser sources coupled with frequency extension in nonlinear crystals.

III. CONCLUSION

The current research efforts in the Byer group are focused on laser development and tunable source development with applications to remote sensing. The laser research and development effort in the past led to the concept and development of the unstable resonator Nd:YAG. The Nd:YAG unstable resonator source has now become a primary research tool in tunable laser applications and in particular, in remote sensing. Our current research efforts focus on the slab geometry lasers and the improved performance allowed by the slab geometry. Our research to date demonstrates that slab geometry lasers should allow an order of magnitude improvement in the average power in pulse energy available from solid state laser sources. The improvement is significant in that it would permit remote sensing measurements that heretofore have not been possible to achieve. For many remote measurements frequency tuning or conversion of frequency tunable sources to new wavelength ranges is essential. An important part of our

on-going research effort is the investigation of tunable solid state laser sources or tunability through parametric oscillator devices. We have made significant advances during the past year in the growth of AgGaS_2 and AgGaSe_2 crystals for use inparametric devices in the infrared spectral range. These chalcopyrite crystals also phasematch for second, third, and fourth harmonic generation of CO_2 lasers and can allow frequency extension of CO_2 TEA lasers to the near infrared spectral range.

We expect to continue our research in slab geometry lasers with emphasis on improved efficiency, reliability and efficient frequency extension at high average power levels. We also expect to extend our slab geometry studies to new laser materials, such as the tunable transitions of chromium in the Gadolinium Gallium Garnet (GGG) crystal host structures.

N.A.S.A. research support has allowed us to take improved laser technology and apply it to remote sensing. The measurement of wind using Nd:YAG technology is an example of this process. We intend to continue our efforts in laser development for applications to remote sensing.

IV.

REFERENCES

1. R.L. Byer, T. Kane, J. Eggleston, Sun, Yuen Long, "Solid State Laser Sources for Remote Sensing", Technical Digest of the Workshop on Optical and Laser Remote Sensing, February 1982, Monterey, California.
2. J.M. Eggleston, T.Kane, J. Unternahrer and R.L. Byer, "Slab Geometry Nd:Glass Laser Performance Studies", Optics Letters, 9, p.405 (1982).
3. K. Kuhn and R.L. Byer, "Conductive Cooling of Slab Glass Laser", Paper WE3, presented at the Optical Society of America Meeting, October 1982, Tucson, Arizona.
4. T. Kane, R.C. Eckardt and R.L. Byer, "Reduced Thermal Focusing and Birefringence in Zig-Zag Slab Geometry Crystalline Lasers", to be published in I.E.E.E. Journal of Quantum Electronics, September 1983
5. T. Kane and R.L. Byer, Patent disclosure submitted June 1983.
6. Sun Yuen Long and R.L. Byer, "Sub-megahertz Frequency Stabilized Nd:YAG Oscillator", Optics Letters, 7, p.408 (1982).
7. L.F. Mollenauer, "Color Center Lasers", in Experimental Physics, Quantum Electronics, vol 15, part B, ed. by C.L. Tang, Academic Press, 1979.
8. P.F. Moulton and A. Mooradian, "Broadly Tunable cw Operation of Ni:MgF₂ and Co:MgF₂ Lasers", Appl. Phys. Letts. 35, p.338 (1979).

9. J.C. Walling, O.G. Peterson and H.P. Jenssen, "Tunable Alexandrite Lasers", IEEE Journal of Quantum Electronics, (November 1980).
10. M. Endemann and R.L. Byer, "Remote Measurements of Trace Species in the Troposphere", A.I.A.A. 19th Aerospace Sciences Meeting, St. Louis, MO. January 1981.
11. S.J. Brosnan and R.L. Byer, "Optical Parametric Oscillator Line-width and Threshold Studies", I.E.E.E. Journal of Quantum Electronics, vol. QE-15, p.415 (1979).
12. Yuan Xuan Fan and R.L. Byer, "AgGaS₂ Optical Parametric Oscillator", presented at the 1983 C.L.E.O. Meeting, (post-deadline paper), Baltimore, Maryland, May 1983.
13. D. Pruss, G. Huber, A. Beinowski and V.V. Laptev, I.A. Shcherbakov, and Y.V. Zharikov, "Efficient Cr⁺⁺⁺ Sensitized Nd⁺⁺⁺ GdScGa Garnet Laser at 1.06 μ m", Applied Physics B 28, Springer-Verlag, p.355 (1982).
14. P.F. Moulton, "New Solid State Tunable Lasers", presented at the 1983 C.L.E.O. Conference, paper ThM1, Baltimore, Maryland, May 1983.

V. PUBLICATIONS AND PRESENTATIONS

Presentations:

Y.K. Fan and R.L. Byer, "An Infrared AgGaS₂ Optical Parametric Oscillator", Post deadline paper - C.L.E.O. Conference, May 1983, held in Baltimore, Maryland.

R.L. Byer, "Progress in Slab Geometry Solid State Lasers", presented in seminar at N.A.S.A. Langely, March 1983.

T.J. Kane and R.L. Byer, "Coherent Doppler Wind Measurements Using Neodymium Lasers", 2nd Conference on Coherent LIDAR held at Aspen, Colorado, August 1983.

Publications:

Appendices, A. B. and C.

Submegahertz frequency-stabilized Nd:YAG oscillator

ORIGINAL PAGE IS
OF POOR QUALITY

Y. L. Sun* and Robert L. Byer

Applied Physics Department, Stanford University, Stanford, California 94305

Received May 7, 1982

We have demonstrated a 5-msec, quasi-cw 10-Hz repetition-rate pulsed single-frequency Nd:YAG oscillator with a feedback-stabilized frequency bandwidth of less than 200 kHz.

Frequency-stabilized, single-mode Nd:YAG is potentially a useful laser source for high-resolution sub-Doppler nonlinear spectroscopy¹ and for atmospheric wind-velocity measurements by coherent lidar Doppler velocimetry.^{2,3} The remote wind measurements require a laser source with less than 1-MHz linewidth and a 1-J, 1- μ sec-duration transmitted pulse. A local oscillator with a 1-mW, 5-msec duration pulse for heterodyne detection of the return signal at up to a 700-km measurement range is also needed for eventual satellite-based global wind measurements. During the past year we have pursued the design of a single-axial-mode Nd:YAG oscillator with the goal of achieving submegahertz frequency stability for applications to nonlinear spectroscopy and remote wind-velocity measurements.

Early work on single-frequency Nd:YAG demonstrated that cw lamp-pumped oscillators could be operated in a stable single axial mode.^{4,5} Typically, measured frequency stabilities were ± 30 MHz at the 100–200-mW cw output-power level. Recent work concentrated on obtaining single-axial-mode output from Q-switched oscillators pumped by pulsed flashlamp excitation.^{6–9} Reasonably stable single-axial-mode selection was demonstrated, but long-term stable-mode selection proved difficult to achieve.

The use of injection locking¹⁰ led to stable single-axial-mode operation of the high-power unstable-resonator Nd:YAG source.¹¹ However, the 10-nsec, Q-switched pulse length limited the injected oscillator bandwidth at 1.064 μ m to 50 MHz. Measurements showed, however, that the master oscillator with a 4- μ sec-duration pulse operated with a frequency chirp that was less than the 9-MHz resolution of the interferometric wavelength analyzer. Thus there was a possibility that linewidths of less than 1 MHz could be achieved in a properly designed oscillator.

We have designed and constructed a quasi-cw flashlamp-pumped, short-cavity TEM₀₀-mode Nd:YAG oscillator. Figure 1 is a schematic drawing of the oscillator, which has a physical cavity length of 8 cm. The 3.0-cm-long 3-mm-diameter Nd:YAG rod and the internal 1-cm-long LiNbO₃ phase modulator result in a cavity optical length of 12 cm and an axial mode spacing of 1.25 GHz. A single axial mode is selected with a 2-mm-thick, finesse-of-seven, solid fused-silica tilted

etalon. The resonator length is controlled by a piezoelectric-crystal-driven mirror and by the internal LiNbO₃ modulator. The laser output beam is well polarized because of the presence of the Brewster plate or, when that is removed, because of the difference in the optical quality for waves with ordinary (high-quality) and extraordinary (low-quality) polarization in the LiNbO₃ crystal. Spatial hole burning is eliminated by two quarter-wave plates placed at each end of the Nd:YAG rod.¹² The entire laser structure is temperature stabilized by temperature-controlled circulating water.

The quasi-cw lamp operation using a krypton-arc lamp was chosen to avoid the power instabilities inherent in tungsten-lamp pumping. Quasi-cw operation also reduced the required average lamp power from 1000 to only 60 W. This in turn significantly reduced the thermal loading on the Nd:YAG rod, thus giving improved laser stability. At the beginning of each quasi-cw pulse, the laser spikes. The spiking pulses decay exponentially in 350 μ sec to a constant 100-mW cw laser output.

The flashlamp is simmered and pulsed for 5 msec at a 10-Hz repetition rate. The flashlamp current must be increased during the pulse to maintain constant laser-output power, as was noted by Kuizenga.¹³

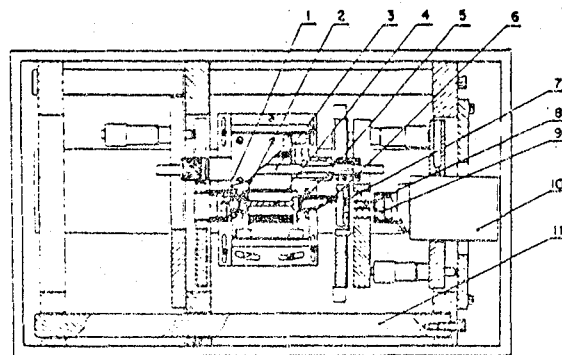


Fig. 1. Schematic of the single-axial-mode Nd:YAG oscillator showing resonator mirrors (1, 9), Nd:YAG rod (4), quarter-wave plates (2, 5), flashlamp (3), Brewster polarizer (6), étalon (7), LiNbO₃ phase modulator (8), piezoelectric stack (10), and Invar resonator spacers (11).

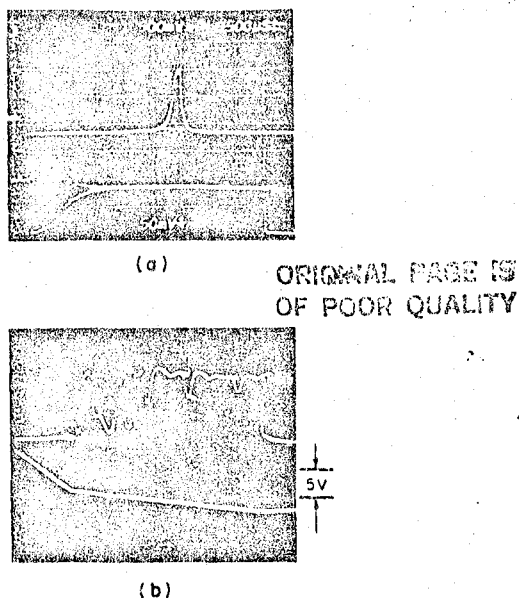


Fig. 2. (a) Upper trace is the 1.06- μm signal transmitted by the 10-cm confocal interferometer as a function of time showing the chirp. The lower trace is the laser output versus time. (b) Upper trace is the 1.06- μm signal transmitted by the 10-cm confocal interferometer with chirp compensation. The amplitude fluctuations indicate residual frequency noise. The lower trace is the voltage applied to the piezoelectric stack versus time showing the initial steep-search voltage ramp followed by the chirp-compensation ramp of 2 V/msec.

Unlike with pure-cw operation, there are two major problems that must be solved to achieve frequency stabilization for quasi-cw operation. The first problem is the frequency chirp caused by periodic pumping and heating of the Nd:YAG rod. We measured the chirp rate by monitoring the laser power transmitted through a 10-cm, high-finesse confocal-interferometer spectrum analyzer. The position of the transmitted peak, shown in Fig. 2(a), can be measured versus bias voltage on the piezoelectric stack of the resonator to yield an accurate value of the chirp rate. The measurement showed a 30-kHz/ μsec chirp rate that is constant on a pulse-to-pulse basis. The chirp can be compensated for, as shown in Fig. 2(b), by applying a 2-V/msec ramp voltage on the resonator piezoelectric stack. Figure 2(b) shows that the residual frequency deviations are 15 MHz. A close look at the remaining frequency fluctuations shows that they are composed of a reproducible (on a pulse-to-pulse basis) high-frequency component that is due to acoustic ringing of the piezoelectric stack and a low-frequency random fluctuation that is caused by the circulating water.

The second problem for quasi-cw operation is that the feedback-control signal is not continuously available. To solve this difficulty and overcome the frequency jitter between pulses and long-term frequency drift, we have developed a special locking system, shown schematically in Fig. 3, which employs a novel search technique to reset the laser wavelength to the confocal-in-

terferometer peak at the beginning of each laser pulse. The search process involves backstepping the voltage on the piezoelectric stack at the end of a pulse and initiating a ramp at the beginning of the next pulse [shown in the lower trace of Fig. 2(b)]. The ramp sweeps the wavelength until the detector senses the laser signal transmitted by the interferometer. The piezoelectric voltage is then switched to the chirp-compensation ramp voltage to compensate for the chirp during the rest of the pulse period.

A second wide-bandwidth feedback loop monitors the power transmitted through the confocal interferometer and provides feedback to the LiNbO₃ phase modulator. This loop locks the laser wavelength to the side of the interferometer peak. For open-loop operation with search and chirp compensation, the laser-frequency deviation, shown in Fig. 4(a), is about 15 MHz.

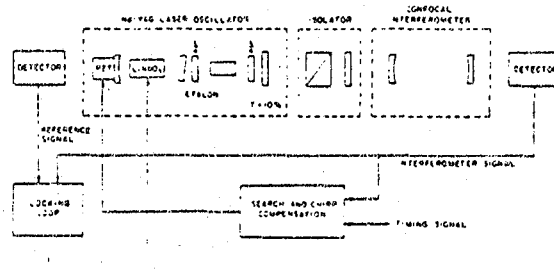


Fig. 3. Laser-frequency-stabilization schematic showing the search and chirp-compensation loop and the wide-bandwidth locking loop using the LiNbO₃ phase modulator.

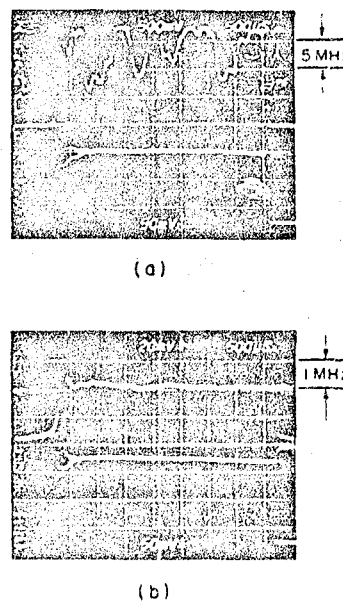


Fig. 4. (a) Open-loop frequency stability with chirp compensation showing frequency fluctuations after chirp compensation. The lower trace is the laser output power versus time. (b) Closed-loop frequency stability showing frequency variations of less than 200 kHz for the 3.5-msec pulse duration. The lower trace is the laser output power versus time.

Closed-loop measurements shown in Fig. 4(b) demonstrate that the frequency stability is enhanced significantly, and the laser-output linewidth is reduced to less than 200 kHz. The search and subsequent locking system ensures that frequency-stabilized single-mode operation is achieved on every pulse. The system has the ability to relocate the lock position even after turned off for short periods and has operated continuously for many hours. Work is in progress to eliminate the piezoelectric ringing and to reduce the laser linewidth further.

In the future, absolute wavelength stabilization may be achieved by frequency doubling in warm phase-matching LiNbO_3 (Ref. 14) and by locking the second harmonic to a hyperfine component¹⁵ of one of the iodine-absorption transitions.⁷

For applications in high-resolution nonlinear spectroscopy and in atmospheric wind measurements, a short part of the 5-msec quasi-cw Nd:YAG output must be sliced with a Pockels-cell switch and amplified. We have demonstrated a gain of 600 in a double-pass Nd:YAG preamplifier. The demonstration experiment utilized a double-pass KD*P Q-switch crystal for pulse-width selection, followed by a double-pass 4-mm-diameter amplifier rod pumped by a pulsed flashlamp. The high gain and reasonable energy storage of Nd:YAG is an important advantage for the laser-amplifier system. We expect to achieve greater than 500 mJ of energy in a 1- μ sec pulse at a 10-Hz repetition rate following a 6.3-mm-diameter saturated final amplifier.

In conclusion, we have demonstrated operation of a stabilized single-axial-mode Nd:YAG oscillator with a frequency bandwidth of less than 200 kHz. The quasi-cw oscillator provides 100 mW of power for a 5-msec-duration pulse at a 10-Hz repetition rate. Further reduction in the linewidth, limited by Fourier transform and shot-noise considerations, appears possible. The frequency-stabilized oscillator, followed by a Nd:YAG amplifier, is a nearly ideal, all-solid-state laser source for atmospheric wind-velocity measurements by coherent Doppler lidar. It should also have applications in high-resolution nonlinear spectroscopic studies at Fourier-transform-limited linewidths.

This research was supported by grants from the U.S. Army Research Office under contract #DAAG29-81-C-0038, the National Aeronautics and Space Administration under grant #NAG1-182, and General Motors Research and Development Laboratories.

* Visiting scholar from North China Research Institute of Electro-Optics, Peking, China.

References

1. R. L. Byer, M. Duncan, E. Gustafson, P. Oesterlin, and F. Konig, "Pulsed and cw molecular beam CARS spectroscopy," in *Laser Spectroscopy V*, A. R. W. McKellar, T. Oka, and B. P. Stoicheff, eds. (Springer-Verlag, Berlin, 1981), p. 233.
2. R. M. Huffaker, "Feasibility of global wind measuring satellite system (WINDSAT)"; R. D. McPerson, "Data requirements and priorities for operational global forecasting during the 1980's and 1990's," in *Digest of Topical Meeting on Coherent Laser Radar for Atmospheric Sensing* (Optical Society of America, Washington, D.C., 1980).
3. R. L. Byer, T. Kane, J. Eggleston, and Y. L. Sun, "Solid state laser sources for remote sensing," presented at the Remote Sensing Conference, Monterey, California, February 1982.
4. H. G. Danielmeyer, "Stabilized efficient single frequency Nd:YAG laser," *IEEE J. Quantum Electron.* QE-6, 101 (1970).
5. W. Culshaw, J. Kanneland, and J. E. Peterson, "Efficient frequency doubled single frequency Nd:YAG laser," *IEEE J. Quantum Electron.* QE-10, 253 (1974).
6. D. C. Hanna, B. L. Davies, and R. C. Smith, "Single longitudinal mode selection of high power actively Q-switched laser," *Opto-Electronics* 4, 249 (1972).
7. R. L. Byer, R. L. Herbst, and R. N. Fleming, "A broadly tunable IR source," in *Laser Spectroscopy*, S. Haroche, J. C. Pebay-Peyroula, T. W. Hansch, and S. E. Harris, eds. (Springer-Verlag, Berlin, 1975), p. 207.
8. A. L. Egorov, V. V. Korobkin, and R. V. Serov, "Single frequency Q-switched neodymium laser," *Sov. J. Quantum Electron.* 5, 291 (1975).
9. Y. K. Park and R. L. Byer, "Electronic linewidth narrowing method for single axial mode operation of Q-switched Nd:YAG lasers," *Opt. Commun.* 37, 411 (1981).
10. Y. K. Park, G. Giuliani, and R. L. Byer, "Stable single-axial-mode operation of an unstable-resonator Nd:YAG oscillator by injection locking," *Opt. Lett.* 5, 96 (1980).
11. R. L. Herbst, H. Komine, and R. L. Byer, "A 200-mJ unstable resonator Nd:YAG oscillator," *Opt. Commun.* 21, 5 (1977).
12. V. Evtuhov and A. E. Siegman, "A twisted mode technique for obtaining axially uniform energy density in a laser cavity," *Appl. Opt.* 4, 142 (1965).
13. D. J. Kuizenga, "Short pulse oscillator development for the Nd:Glass laser fusion system," *IEEE J. Quantum Electron.* QE-17, 1694 (1981).
14. R. L. Byer, Y. K. Park, R. S. Feigelson, and W. L. Kway, "Efficient second harmonic generation of Nd:YAG laser radiation using warm phase-matching LiNbO_3 ," *Appl. Phys. Lett.* 39, 17 (1981).
15. M. D. Levenson, "Hyperfine interactions in molecular iodine," Ph.D. Thesis (Stanford University, Stanford, California, 1971).

ORIGINAL PAGE IS
OF POOR QUALITY

APPENDIX B

6.2 Solid-State Laser Sources for Remote Sensing

R.L. Byer, T. Kane, J. Eggleston, and Sun Yun Long*

Stanford University, Ginzton Laboratory, Stanford, CA 94305, USA

4. O. Uchino, H. Maeda, J. Kohno, T. Shibata, C. Nagasawa, and M. Hirono, *Appl. Phys. Lett.* **33**, 607 (1978).
5. H. Nicolet, "An Overview of Aeronomic Processes in the Stratosphere and Mesosphere," *Can. J. of Chem.* **52**, 1381 (1974).
6. E. L. Baardsen and R. W. Terhune, *Appl. Phys. Lett.* **21**, 209 (1972).
7. C. C. Wang and L. I. Davis, *Phys. Rev. Lett.* **32**, 349 (1974).
8. D. D. Davis, W. Heaps, and T. McGee, *Geophys. Res. Lett.* **3**, 331 (1976).
9. W. Heaps, unpublished.
10. W. S. Heaps, *Appl. Opt.* **19**, 243 (1980).
11. T. McKee, *Phys. in Can.* **36**, 41 (1979).
12. T. J. Pacala, I. S. McDermid, and J. B. Laudenslager, *Appl. Phys. Lett.* **40**, 1 (1982).
13. H. A. A. Clyne and I. S. McDermid, *Laser Induced Fluorescence: Electronically Excited States of Small Molecules*, *Advances in Chemical Physics* edited by K. P. Lawley (John Wiley & Sons, England, in press).

I. INTRODUCTION

Remote sensing with laser sources has made tremendous strides during the past decade. The progress has been paced, however, by the slow development of the high power, narrow bandwidth, tunable laser sources required as transmitters for DIAL and coherent detection methods. Only recently, with the development of Nd:YAG pumped dye and parametric oscillator sources has near infrared and ultraviolet measurement systems been demonstrated.

This paper summarizes recent progress in solid state lasers that utilize the slab geometry with a zig-zag optical path as illustrated in Fig. 1.

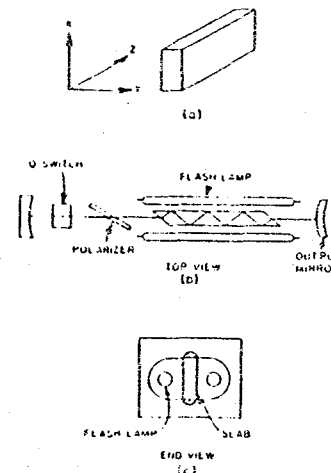


Figure 1.
 a--Geometry showing axis of the slab.
 b--Schematic of the laser resonator with Brewster angle slab and zig-zag optical path.
 c--End view of the slab holder showing flashlamp position within the non-imaging flashlamp reflector structure

The slab configuration solid state laser approach first proposed and investigated at General Electric¹ has been under development in our laboratory for the past three years. Slab geometry lasers offer a number of important advantages over the conventional rod geometry lasers. These advantages include the elimination of stress induced birefringence and thermal and stress induced focusing, and higher average output power limited only by stress induced fracture of the glass or crystalline laser host material. The progress in slab Nd:Glass and Nd:YAG lasers is discussed in Section II.

Coherent detection of wind velocity by Doppler velocimetry has now been established as a viable measurement approach at the CO₂ laser infrared wavelength range.² We have undertaken

* Visiting scholar from North China Electro-Optics Institute, Peking, China.

to design a single frequency Nd:YAG laser source for coherent wind velocity measurements at 1.00 μm . The Nd:YAG source offers the potential advantages compared to CO_2 based system of more than two orders of magnitude larger backscatter coefficient, improved depth resolution, room temperature silicon diode based detection and a compact all solid state construction. The design and testing of a single frequency Nd:YAG oscillator is discussed in Section III.

II. SLAB GEOMETRY SOLID STATE LASERS

A. Introduction

Remote atmospheric measurements using the DIAL technique requires a high pulse energy tunable laser source. Only recently, with the development of the unstable resonator Nd:YAG source³ has 1 J pulse energies at 10 Hz repetition rate become available. However, the Nd:YAG pumped 1.4-4.0 μm tunable parametric oscillator source⁴ has been limited to 10-50 mJ of output energy. The doubled Nd:YAG pumped dye tunable source has output pulse energies up to 100 mJ. For SO_2 measurements in the ultraviolet, the doubled dye laser output energy is typically 10 mJ.^{5,6} These energies are adequate for range resolved measurements over intermediate ranges, but are an order of magnitude below the requirements for space shuttle based LIDAR or DIAL measurements to 10 kilometer ranges. In addition, from a system viewpoint, the tunable OPO or dye laser is not as efficient or reliable as desired for long term measurement applications.

We began our slab geometry laser development effort three years ago in recognition of the need for a higher pulse energy, more reliable tunable source. Our approach was to tune the glass laser over its 200 cm^{-1} wide bandwidth and to extend the tuning range by harmonic generation and by selective Raman shifting.⁷

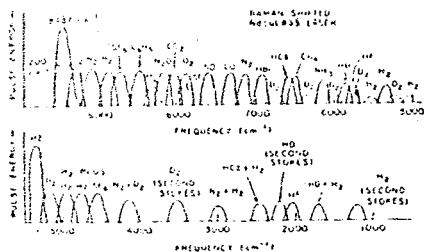


Figure 2--Tuning range of Nd:Glass laser centered at 1.055 μm followed by Raman shifting in gases. Harmonic generation in LiNbO_3 and $\text{KH}_2\text{P}_2\text{O}_7$ can be used to extend the wavelength range into the visible and ultraviolet range

Figure 2 illustrates the tuning range available with just a few Raman active gases. Harmonic generation can be used to extend the tuning range into the ultraviolet and visible spectral regions. The tunable Nd:Glass oscillator/amplifier source, followed by nonlinear frequency extension, combines the higher pulse energies generated in Nd:Glass with solid state reliability and system simplicity. The key to successful implementation lies in the application of the slab geometry concept.

To appreciate the advantages of the

zig-zag slab geometry approach it is useful to compare the performance limitations of rod geometry lasers to slab geometry lasers. To make the comparison specific we consider the performance limits of a 15 cm long x 6 mm diameter Nd:Glass rod laser and a 15 cm long x 8 mm thick three-to-one aspect ratio slab Nd:Glass laser.

The performance limitations are summarized in Table I for LiG-8 phosphate glass. Phosphate glass was selected because of its high gain cross-section and negative dn/dT which helps to offset thermal and stress focusing in the rod laser.

TABLE I Rod and Slab Geometry Laser Design Limitations

Rod geometry (5 mm dia. x 15 cm length LiG-8 phosphate glass)	Average flashlamp power. (Watts)	Effect
Birefringence	100	π phase shift
Thermal focusing	1000	-115 cm focal length
Stress focusing	1000	+70 cm focal length (biaxial)
Stress fracture	1000	Surface stress fracture limit
Slab geometry (8.3 mm x 25 mm x 15 cm length, LiG-8 phosphate glass)		
Birefringence	-	Eliminated by zig-zag geometry
Thermal & stress focusing	-	Eliminated by zig-zag optical path
Stress fracture	2000	Only design limitation

In the rod geometry, the stress fracture limit occurs at 5 Hz repetition rate at 200 J flashlamp energy or 1000 W of average input power. This stress fracture limit was verified experimentally by fracturing rods of Nd:Glass. Stress and thermal focal lengths are +70 cm and -115 cm at the stress fracture loading limit. These focusing effects must be compensated in the design of the laser oscillator to enable near diffraction limited performance. Since the stress and thermal focusing has both radial and tangential components, the focusing is not equivalent to a lens but is instead a biaxial focusing element that cannot be simply compensated by an additional lens.⁸

Finally, at 1/2 Hz repetition rate, or 100 W of flashlamp average power, stress induced birefringence is severe enough to cause a polarization induced phase shift of π radians. This in turn induces a severe loss for linearly polarized resonator designs that are required for Q-switching or frequency extension by nonlinear processes.

The slab geometry, on the other hand, completely eliminates stress induced birefringence by slab symmetry. If a zig-zag optical path is used, then the stress and thermal induced focusing is also eliminated. This leaves stress fracture as

QUALITY OF PAPER GUARANTEED

the only design limitation on the average power loading of the slab and thus on the available average output power. For IRG-8 glass, the thermal loading limit set by fracture induced birefringence is 2000 W for an 8.2 mm x 25 mm x 15 cm glass slab. At this loading, the slab can operate at up to 5 Hz repetition rate and store up to 2 J of optical energy at 1.75% storage efficiency. Clearly the slab geometry offers a significant performance improvement over the usual rod geometry approach.

B. Nd:Glass slab measurements

The advantages of the zig-zag slab geometry have been known for more than a decade.¹ Only recently, however, has the technology for fabricating the slabs become widely available. The demands of the laser fusion research effort have pushed the fabrication and optical coating technology to the present status where slab fabrication is possible at a reasonable cost.

To take full advantage of the slab geometry in laser system design, we have developed a computer program that calculates the thermal profile of the slab, the induced stresses, the stress induced depolarization, and ray traces the zig-zag optical path through the slab. The program displays the results and can be used as an interactive design tool.

To be useful the computer model must be carefully calibrated and verified. We have accomplished verification, where possible, by comparison with analytical solutions to the thermal and stress equations. However, a test-bed Nd:Glass slab laser source was designed and constructed to provide calibration and quantitative verification of the model. Measurements using the test-bed laser system have verified predictions of the model and have shown that the slab geometry approach does, in practice, provide the projected advantages of elimination of birefringence and thermal and stress induced focusing.

The calculated stresses in the thermally loaded slab are an example of the model capability. Figure 3 shows the compression and tension field in the slab assuming uniform pumping on the y faces. From the stress field, the depolarization can be calculated and displayed as shown in Fig. 4. Note that the peak depolarization is predicted to be 32% while the average depolarization over the slab area is near 5%. Figure 5 shows a plot of predicted depolarization (solid curve) and measured depolarization (dots) at 1600 W average flashlamp power loading of the slab.¹⁰ The excellent agreement verified a number of aspects of the model including the calculated stress field, depolarization and optical ray tracing along the zig-zag path.

Using the slab test-bed laser we have completed measurements of gain, energy storage efficiency, pumping uniformity, depolarization, beam divergence and quality, thermal induced end effects and coolant effects on focusing, tuning,

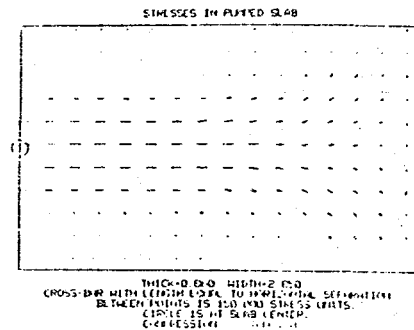


Figure 3--Calculated tensional and compressional stresses in a pumped glass slab assuming uniform pumping on the y faces. The slab is in compression in the center and tension at the edges. The tensional stress at the surface eventually leads to fracture of the slab.

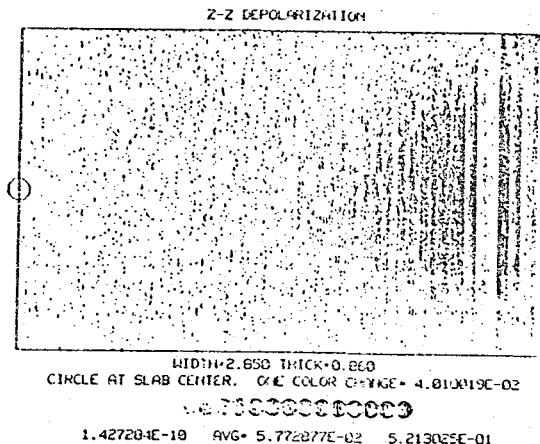


Figure 4--Calculated depolarization for a pumped glass slab assuming uniform pumping on the y faces. The maximum depolarization is near 32%. Note that over a large region of the slab the depolarization is insignificant.

Q-switch oscillator operation, and second harmonic generation.⁹

The test-bed slab laser has operated as a long pulse oscillator at 3.75% storage efficiency, 2.0% slope efficiency and 1.6% wall plug efficiency. Typical output data for extraction from the entire slab volume is shown in Fig. 6a. We have used the test-bed slab laser to verify, by far field diffraction measurements, that the beam quality of the slab is diffraction limited. We have operated a slab glass oscillator using both an unstable resonator³ and a radial birefringent resonator design.¹¹ Figure 6b shows the output pulse energy free running and Q-switched for the 6 mm diameter oscillator mode volume.

We plan to follow the oscillator by a pre-amplifier in the same slab to generate 1.2J and by an amplifier in a second identical slab to generate over 6J per

pulse at 5 Hz repetition rate. We have previously demonstrated tuning over a 100 cm^{-1} range with a prism beam expander and grating. We expect efficient nonlinear frequency extension via SHG and Raman processes due to the diffraction limited polarized output beam quality. The theoretical and experimental results for the slab laser are being prepared for presentation and publication.¹²

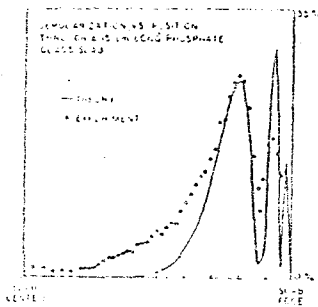


Figure 5--Predicted and measured depolarization for a pumped glass slab. The oscillations are caused by stress vector rotation combined with the zig-zag optical path through the slab

Future slab laser research will involve the completion of a second generation slab laser system with more efficient flashlamp pumping, an optimized slab thickness and improved resonator/amplifier designs. The improved slab glass laser system will be used in remote sensing measurements in the near infrared.

C. Nd:YAG Slab Laser Measurements

The slab geometry can also be applied to crystalline laser systems. We have carried out preliminary measurements with a cw lamp pumped Nd:YAG slab oscillator. These measurements have shown that thermal and stress induced focusing can be eliminated with the zig-zag slab geometry in Nd:YAG at up to 4 kW of flashlamp average power. This level of pumping is over six times that typically

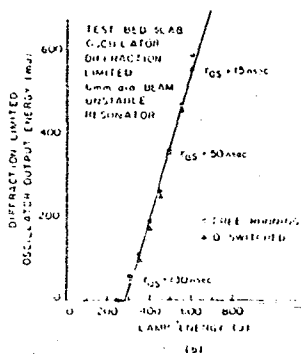
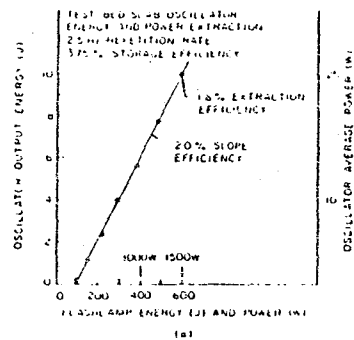


Figure 6.
a--Measured long pulse output energy and average power from the test-bed slab laser vs input flashlamp energy at 2.5 Hz repetition rate. The 1500 W average flashlamp power is below the measured 2000 W stress fracture limit for the present 8.3 mm x 25 mm x 15 cm long LiG-5 glass slab
b--Measured Q-switched output energy for a 6 mm diameter beam, unstable resonator oscillator

used for Q-switched, high power, pulsed Nd:YAG unstable resonator laser systems. The present peeping limit is set by the maximum power provided by our currently available power supply and not by the thermal limitations of the Nd:YAG slab.

We have also verified that the slab geometry completely eliminates stress induced birefringence in Nd:YAG.¹³ This is important for applications where Nd:YAG is to be frequency shifted by nonlinear processes. Work is continuing on the slab geometry applied to crystalline laser host materials.

In summary, the slab geometry approach offers more than an order of magnitude improvement in laser performance for both Nd:Glass and Nd:YAG laser systems. Recent model and test-bed laser experiments have verified that the expected improvements are realizable in practice.

III. SINGLE FREQUENCY Nd:YAG OSCILLATOR/AMPLIFIER SYSTEM

A. Introduction

The tremendous progress of coherent LIDAR measurements at the CO₂ wavelength range² has sparked an interest in long range depth resolved wind measurements and coherent LIDAR. An examination of the measurement system shows that there are advantages to be gained by using wavelengths shorter than 10 μm . These advantages include increased backscatter by more than two orders of magnitude at 1 μm as opposed to 10 μm , improved depth resolution, access to room temperature silicon diode detectors with avalanche gain, and solid state transmitters with demonstrated long operational lifetimes and small volume and weight. The principal difficulty in the approach to shorter wavelength coherent LIDAR measurements was the unknown bandwidth of the transmitter due to the unknown thermally induced chirp rate in the solid state laser host material.

During the past year we have pursued the design of a single axial mode Nd:YAG oscillator with the goal of demonstrating a frequency stability adequate for wind velocity measurements by Doppler velocimetry in the atmosphere.

B. Nd:YAG Oscillator Design

Our research efforts with single frequency Nd:YAG oscillators has clearly shown that Nd:YAG is not homogeneously saturated and that special steps such as injection locking¹⁴ must be taken to insure single mode operation. We also learned previously that the Nd:YAG chirp rate was less than 9 MHz for pulsed flashlamp excitation. Thus there was a possibility that the chirp rate in Nd:YAG could, in fact, be much less than 9 MHz and that linewidths of less than 1 MHz required for wind measurements could be achieved.

We have designed a quasi-cw flashlamp pumped, very short cavity, Nd:YAG TEM₀₀ mode oscillator source to test the frequency linewidth limitations. The oscillator is shown schematically in Fig. 7. The cavity physical length is 7.5 cm. The

ORIGINAL PAGE IS OF POOR QUALITY

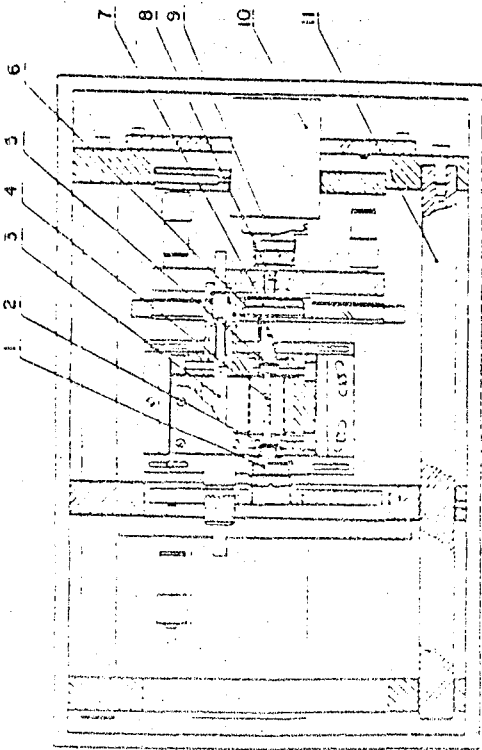


Figure 7-- Schematic of the single axial mode Nd:YAG oscillator showing resonator mirrors (1, 2), YAG rod (3), quarter wave plates (4, 5), flashlamp (6), Brewster polarizer (7), LiNbO₃ phase modulator (8), piezoelectric stack (9), and invar resonator spacers (10, 11). The resonator optical length is 10 cm due to the 2.0 cm Nd:YAG rod and thus the axial mode spacing is 1.5 MHz. A single 2 mm thick fused silica tilted etalon, with a finesse of 7 is adequate to select a single axial mode under the very broad 10 cm⁻¹ Nd:YAG gain curve.

The flashlamp is dimmed and pulsed for a 3-5 msec period at 10 Hz repetition rate. To generate constant power output during the quasi-cw pumping period, the flashlamp current must be increased during the pulse as shown in Fig. 8a. Note that the laser oscillator initially spikes when threshold is reached, but that the spiking behavior decays to steady state output in 240 nsec as expected.

The laser output frequency can be stabilized relative to the tilted etalon pass band by measuring the output power vs time as originally noted by Kuzenga. The power variation is due to the chirp of the axial mode frequency relative to the etalon pass band and is one approach to determining the chirp rate. The chirp rate can also be measured by monitoring the laser output power after a high resolution confocal interferometer spectrum analyzer as shown in Fig. 8b. The position of the peak can be measured as a function of bias voltage on the piezoelectric stack of the resonator to yield an accurate measurement of the chirp rate. Gain measurements showed that the present Nd:YAG oscillator has a chirp rate of 30 kHz per 1 microsecond.

This chirp rate is very constant from pulse-to-pulse and can be compensated by inducing a ramp voltage of 2 v per millisecond on the laser resonator piezo-

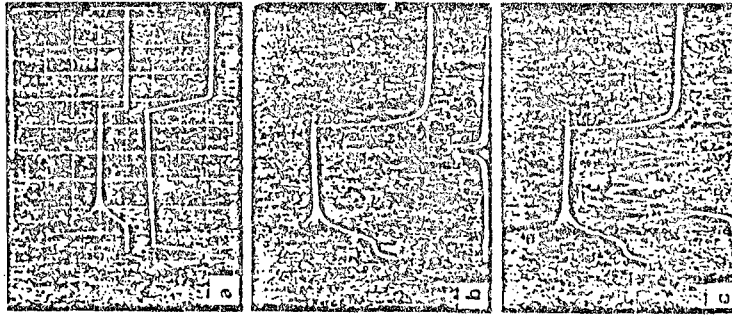


Figure 8a: Upper trace shows the quasi-cw simple axial mode Nd:YAG laser output at 0.1 W power level. The lower trace shows the pumping lamp current with ramp compensation to achieve constant laser output power.

Figure 8b: The upper trace shows the laser output power for the 3 msec pulse. The lower trace shows the output power following a 10 cm, R = 99.7% confocal interferometer spectrum analyzer. Measurement of the pulse width or delay shows that the chirp rate is 30 kHz per microsecond.

Figure 8c: Upper trace is laser output power. The lower trace is the laser power detected after the confocal interferometer while the chirp is compensated by a 2V/msec ramp on the PZT. Acoustically induced vibrations lead to the power and frequency fluctuations which are less than 1-20 MHz on a pulse-to-pulse basis.

electric stack. The result of this procedure is to stabilize the output frequency over the 3 millisecond duration as shown in Fig. 8c. The remaining oscillations in amplitude correspond to acoustic induced cavity length variations that in turn yield a 1-20 kHz pulse-to-pulse frequency stability.

We are in the process of completing a locking loop to stabilize the Nd:YAG output frequency onto a 10 cm confocal interferometer with a 15 MHz passband. We expect to demonstrate a closed loop frequency stability of less than 1 MHz using a combination of a 1 kHz bandwidth feedback to the piezoelectric controlled mirror and a 1 MHz bandwidth feedback to a LiNbO₃ phase modulator within the Nd:YAG oscillator cavity.

The 3 millisecond quasi-cw operation was selected so that an early part of the output could be selected by a half-wave electro-optic switch and amplified by a Nd:YAG amplifier chain. The remaining part of the pulse is then available for use as the local oscillator for the heterodyne measurement for ranges up to 400 km. Longer pulse lengths are easily possible so that measurements from space platforms at 1000 km altitude are feasible. The quasi-cw operation significantly reduces the

ORIGINAL COPY IS OF POOR QUALITY

power consumption of the oscillator. The present system requires 30 W average power into the flashlamps while a cw lamp pumped oscillator could require close to 1000 W to achieve the same performance.

The present Nd:YAG oscillator generates 0.1 W of output power. We have demonstrated a double pass amplifier with a gain of 600 that utilized a 4 mm diameter Nd:YAG rod pumped by a pulsed flashlamp. We have verified that the laser linewidth is not broadened by the pre-amplifier. We expect, in the future, to demonstrate amplification to pulse energies of greater than 300 mJ in a 1 micro-second pulse at 10 Hz repetition rate in a rod geometry Nd:YAG system. The use of slab geometry offers an order of magnitude improvement without sacrificing beam quality or frequency stability.

In summary, we have demonstrated that a single frequency Nd:YAG oscillator operating in a Q-switched mode has a chirp rate of 30 kHz per microsecond and a line running stability of ± 20 MHz. The chirp can be easily compensated thus giving adequate frequency stability for wind velocity measurements by coherent LIDAR.

We plan to pursue the Nd:YAG source improvements and to apply the system to atmospheric wind studies. In the future, diode laser pumped Nd:YAG sources¹⁶ offer the possibility of an efficient, long term operation, space qualified transmitter source for global wind velocity measurements.

IV. CONCLUSION

We have pursued the study of advanced solid state laser concepts with the goal of meeting remote sensing transmitter requirements for future LIDAR systems. The frequency shifted, tunable glass laser source, using the slab geometry approach, offers the potential for a high pulse energy, high average power solid state transmitter without the need for a parametric oscillator or dye laser tunable source. The current Stanford test-bed slab laser source has a design goal of 6 J per pulse at 5 Hz with greater than 1% wall plug efficiency. Advanced slab glass laser designs, such as the system presently under construction at the Swiss Institute of Nuclear Research for measurements at 6.0 μ m wavelength of the Lamb shift in the α hydrogen atom,¹⁶ call for 10 J of output energy at 50 Hz repetition rate or 500 W of average output power. Clearly these next generation laser sources will have a major impact on the tunable LIDAR measurement capability.

The demonstration of a small chirp rate in a Nd:YAG single axial mode oscillator opens the possibility for remote wind measurements by coherent LIDAR at 1.06 μ m. The advantages of shorter wavelength and an all solid state transmitter offer the possibility of global wind field measurements from satellite platforms.

ACKNOWLEDGEMENTS

We want to acknowledge the support provided by the United States Army Research Office through contract number DAAO19-81-C-0038, the Department of Energy through contract number DOE J819301 and by the National Aeronautics and Space Administration through contract number NAO1-182. We also want to acknowledge the early contributions to this work by Dr. J. Unternahrer of the Swiss Institute of Nuclear Research.

REFERENCES

1. W.S. Martin and J.P. Chernock, "Multiple Internal Reflection Face Pumped L. U.S. Patent #3,633,126, (1972); see also, Y.S. Liu, W.B. Jones and J.P. Chernock, "Recent Development of High Power Visible Laser Sources Employing Solid State Slab Lasers and Nonlinear Conversion Techniques", General Electric Report #BICRD104, May 1981.
2. R. Milton Huffaker, "Feasibility of a Global Wind Measuring Satellite System (WINDSAT)"; and also R.D. McPerson, "Data Requirements and Priorities for Operational Global Forecasting During the 1980's and 1990's" in the Proceedings of the Coherent Laser Radar for Atmospheric Sensing Conference held at Aspen Colorado, July 1980.
3. R.L. Herbst, H. Kamine and R.L. Byer, "A 200 mJ Unstable Resonator Nd:YAG Oscillator", *Optics Commun.* 21, p.5 (1977); see also R.L. Byer, "Nd:YAG Pumped Tunable Sources and Applications", (to be published).
4. M. Endemann and R.L. Byer, "Remote Single Ended Measurements of Atmospheric Temperature and Humidity at 1.9 μ m Using a Continuously Tunable Source", *Optics Letters*, vol. 5, October 1980; see also M. Endemann and R.L. Byer, "Remote Measurement of Trace Species in the Troposphere", presented at the A.I.A.A. 19th Aerospace Sciences Meeting, January 12-15, 1981, St. Louis, Missouri, (to be published).
5. J.G. Hawley, G.F. Wallace, L.D. Fletcher, "A Mobile Differential Absorption Lidar (DIAL) for Range Resolved Measurements of SO₂, O₃ and NO₂", presented at the A.I.A.A. 19th Aerospace Sciences Meeting, January 12-15, 1981, St. Louis, Missouri.
6. K. Fredrikson, B. Calle, K. Mystrom and S. Svamberg, "Mobile LIDAR System for Environmental Probing", *Applied Optics*, vol. 20, p.4181 (1981).
7. R.L. Byer, "Frequency Conversion via Stimulated Raman Scattering", *Electro-Optical Systems Designs*, February 1980.
8. W. Koechner and D.K. Rice, "Birefringence of Nd:YAG Laser Rods", *J. Opt. Soc. Am.* 61, p.758 (1971).
9. J.M. Eggleston, "Theoretical and Experimental Studies of Slab Geometry Lasers", Ph.D. Thesis, Stanford University, April 1982.

ORIGINAL PAGE IS
OF POOR QUALITY



REDUCED THERMAL FOCUSING AND BIREFRINGENCE

IN ZIGZAG SLAB GEOMETRY CRYSTALLINE LASERS

T J KANE, R C ECKARDT and R L BYER

ORIGINAL PAGE IS
OF POOR QUALITY

ABSTRACT: Replacing the rod in a Nd:YAG laser with a zigzag slab resulted in a very substantial reduction of the thermally induced optical distortion without sacrifice of output power or efficiency. This reduction was possible after simple measures were taken to eliminate end and edge effects.

In this letter we present interferometric measurements of the thermally induced optical effects in laser crystals cut in both the zigzag slab and the conventional rod geometries. These measurements confirm the present understanding of zigzag slab geometry lasers and demonstrate the significant advantages obtained by replacing the rod in a Nd:YAG laser with a slab. We describe simple measures to eliminate end and edge effects and present efficiency and threshold data for the Nd:YAG slab and the rod it replaced.

In conventional cylindrical rod solid state lasers, both temperature and thermally induced stress change the index of refraction, and the laser beam is distorted. The rod becomes a non-uniform multi-wave birefringent element and a strong and polarization-dependent lens. These effects have been thoroughly described and analyzed [1-4].

The zigzag slab laser geometry, also known as the total internal reflection face pumped laser geometry, was invented by Martin and Chernoch at General Electric [5]. This geometry greatly reduces the thermally induced optical effects in the pumped laser [6,7]. The zigzag slab geometry is shown schematically in Fig. 1. Focussing is eliminated in the x direction by the uniformity of the pumping and cooling in that direction, and in the y

APPENDIX C

REDUCED THERMAL FOCUSING AND BIREFRINGENCE

IN ZIGZAG SLAB GEOMETRY CRYSTALLINE LASERS

ORIGINAL PAGE IS
OF POOR QUALITY

T J KANE, R C ECKARDT and R L BYER

ABSTRACT: Replacing the rod in a Nd:YAG laser with a zigzag slab resulted in a very substantial reduction of the thermally induced optical distortion without sacrifice of output power or efficiency. This reduction was possible after simple measures were taken to eliminate end and edge effects.

In this letter we present interferometric measurements of the thermally induced optical effects in laser crystals cut in both the zigzag slab and the conventional rod geometries. These measurements confirm the present understanding of zigzag slab geometry lasers and demonstrate the significant advantages obtained by replacing the rod in a Nd:YAG laser with a slab. We describe simple measures to eliminate end and edge effects and present efficiency and threshold data for the Nd:YAG slab and the rod it replaced.

In conventional cylindrical rod solid state lasers, both temperature and thermally induced stress change the index of refraction, and the laser beam is distorted. The rod becomes a non-uniform multi-wave birefringent element and a strong and polarization-dependent lens. These effects have been thoroughly described and analyzed [1-4].

The zigzag slab laser geometry, also known as the total internal reflection face pumped laser geometry, was invented by Martin and Chernock at General Electric [5]. This geometry greatly reduces the thermally induced optical effects in the pumped laser [6,7]. The zigzag slab geometry is shown schematically in Fig. 1. Focussing is eliminated in the x direction by the uniformity of the pumping and cooling in that direction, and in the y

9. J.C. Walling, O.G. Peterson and H.P. Jenssen, "Tunable Alexandrite Lasers", IEEE Journal of Quantum Electronics, (November 1980).
10. M. Endemann and R.L. Byer, "Remote Measurements of Trace Species in the Troposphere", A.I.A.A. 19th Aerospace Sciences Meeting, St. Louis, MO. January 1981.
11. S.J. Brosnan and R.L. Byer, "Optical Parametric Oscillator Line-width and Threshold Studies", I.E.E.E. Journal of Quantum Electronics, vol. QE-15, p.415 (1979).
12. Yuan Xuan Fan and R.L. Byer, "AgGaS₂ Optical Parametric Oscillator", presented at the 1983 C.L.E.O. Meeting, (post-deadline paper), Baltimore, Maryland, May 1983.
13. D. Pruss, G. Huber, A. Beinowski and V.V. Laptev, I.A. Shcherbakov, and Y.V. Zharikov, "Efficient Cr⁺⁺⁺ Sensitized Nd⁺⁺⁺ GdScGa Garnet Laser at 1.06 μ m", Applied Physics B 28, Springer-Verlag, p.355 (1982).
14. P.F. Moulton, "New Solid State Tunable Lasers", presented at the 1983 C.L.E.O. Conference, paper ThM1, Baltimore, Maryland, May 1983.

IV.

REFERENCES

1. R.L. Byer, T. Kane, J. Eggleston, Sun, Yuen Long, "Solid State Laser Sources for Remote Sensing", Technical Digest of the Workshop on Optical and Laser Remote Sensing, February 1982, Monterey, California.
2. J.M. Eggleston, T.Kane, J. Unternahrer and R.L. Byer, "Slab Geometry Nd:Glass Laser Performance Studies", Optics Letters, 9, p.405 (1982).
3. K. Kuhn and R.L. Byer, "Conductive Cooling of Slab Glass Laser", Paper WE3, presented at the Optical Society of America Meeting, October 1982, Tucson, Arizona.
4. T. Kane, R.C. Eckardt and R.L. Byer, "Reduced Thermal Focusing and Birefringence in Zig-Zag Slab Geometry Crystalline Lasers", to be published in I.E.E.E. Journal of Quantum Electronics, September 1983
5. T. Kane and R.L. Byer, Patent disclosure submitted June 1983.
6. Sun Yuen Long and R.L. Byer, "Sub-megahertz Frequency Stabilized Nd:YAG Oscillator", Optics Letters, 7, p.408 (1982).
7. L.F. Mollenauer, "Color Center Lasers", in Experimental Physics, Quantum Electronics, Vol 15, part B, ed. by C.L. Tang, Academic Press, 1979.
8. P.F. Moulton and A. Mooradian, "Broadly Tunable cw Operation of Ni:MgF₂ and Co:MgF₂ Lasers", Appl. Phys. Letts. 35, p.338 (1979).

Table I cont.

<u>Date</u>	<u>Laser System</u>	<u>Performance</u>
August 1982	10cm x .8cm x .4cm Nd:YAG cw lamp pumped (4kW)	80W cw 2% efficiency
November 1983	10cm x .8cm x .4cm Nd:YAG cw lamp pumped (10kW)	200W cw 2% efficiency
December 1983	10cm x .8cm x .4cm Nd:YAG multiplexed slab amplifier	30mJ at 20Hz TEM ₀₀ mode, single axial mode

TABLE I

Slab Laser Demonstrated and Projected Performance

Stanford University

Nd:Glass

<u>Date</u>	<u>Laser System</u>	<u>Performance</u>
October 1981	15cm x 2.5cm x .83cm 3% doped phosphate glass fluid cooled test-bed laser	10J 2.5Hz 1% efficiency 25W average power
October 1982	15cm x 2.5cm x .65cm 8% doped phosphate glass helium conduction cooled	18J 2Hz 2.3% efficiency 36W average power
June 1983	30cm x 4cm x .65cm 8% doped phosphate glass helium conduction cooled longitudinal flashlamps	15J 5Hz 1.5% efficiency 75W average power
December 1983	30cm x 4cm x .65cm 8% doped phosphate glass helium conduction cooled transverse flashlamps	10J 10Hz 3% efficiency 100W average power

direction by the averaging of temperature that takes place over a full zigzag. The birefringence caused by the thermal stress in a slab is also much lower than that of a rod, because the major component of stress averages to zero over a full zigzag. Recently we have built and tested a zigzag geometry Neodymium doped glass laser, developed a computer model of the thermally induced optical effects in slabs, and successfully tested the model [8,9].

For the crystal slab tests described in this letter, we fabricated zigzag slabs of Nd:YAG and Nd:GGG (Gadolinium Gallium Garnet). The material Nd:GGG is of interest because its large change in index of refraction with temperature has been a major reason for its infrequent use in rod geometry lasers. In the slab geometry thermal focussing is fully compensated, so it is possible to take advantage of the superior crystal growth properties and greater resistance to thermal fracture of Nd:GGG. We achieved stable CW operation of the Nd:GGG slab, but a meaningful efficiency comparison is not possible until more highly doped material is available. The Nd:GGG and Nd:YAG slabs were tested in a commercial CW laser system. The laser head contained a single 6-mm inner-diameter krypton arc lamp, with 76 millimeters of radiating length. A gold coated elliptical cavity focussed the pump light into the slab. The slabs were mounted from the ends, and two simple procedures, described below, were used to approach the ideal slab thermal boundary conditions.

To approach the ideal slab limit of zero thermally induced optical distortion, it is necessary to avoid cooling the non-reflective edges, and thus avoid creating a temperature gradient in the x direction. We achieved adequate insulation by the simple means of attaching silicone rubber to the non-reflecting edges of the slab. Dow Corning Sylgard 186, with a thermal conductivity of 0.0017 Watt/cm²*K [10] has 34 times higher thermal resistance

than Nd:YAG. Thus a relatively thin layer (about 1 mm for our 4-mm x 8-mm slabs) effectively insulated the surface.

ORIGINAL PAGE IS
OF POOR QUALITY

The ideal slab appears optically flat in the y direction because all zigzag segments have the same average index of refraction. This is not true near the ends of a finite slab. We observed strong negative focussing in the y direction when the entire slab, including the ends, was pumped. Again, a very simple procedure consisting of slipping opaque tubes over the ends of the slab to shield the entrance face from the flashlamp radiation greatly reduced the negative focussing. In order to use the pump light efficiently while shielding the ends of the slab, it is necessary that the slab be longer than the radiating length of the lamp. Our slab was 100 mm from tip to tip, though the lamp radiating length was 76 mm.

The optical quality of the pumped slab was measured with a Mach-Zehnder interferometer. A 633-nanometer Helium-Neon laser was used as the light source. The location of each fringe was measured on horizontal and vertical cuts through the center of the interference pattern and the fringe number was plotted as a function of distance from the center. A least-square fringe-fitting procedure determined the focal length of the pumped slabs and rods and also gave the residual distortion.

The most complete set of interferograms were taken for the Nd:GGG slab. Interferograms were recorded for four cases: 1) no thermal insulation and no shielding, 2) insulation but no shielding, 3) shielding but no insulation, and 4) with both shielding and insulation. Fig. 2 is a reproduction of these four interferograms at a lamp pumping power of 4.2 kilowatts. Table 1 summarizes the results for the Nd:GGG slab. In the x direction, shielding and insulation changed the thermal focussing from 1.35 diopters to -0.26 diopters. Most of the change in the x direction was due to the insulation.

In the y direction, the change was from -2.34 diopters to -0.46 diopters, with almost all of the improvement due to the shielding. The Nd:GGG measurements clearly show that the slab boundary conditions are critical to the reduction of thermal focussing. The difference between the focussing power in the two directions, a parameter of key importance to resonator stability, was reduced to 5.4% of its original value.

ORIGINAL FILE IS
OF POOR QUALITY

Data for the Nd:YAG slab were recorded for the case where both shielding and insulation were in place. The 4-mm by 8-mm slab used had almost the same cross-sectional area as the 6.4-mm diameter rod it replaced, so a comparison is possible. The interferograms of the Nd:YAG slab and rod at 4.2 kilowatts of lamp power are reproduced in Fig. 3. Table 2 summarizes the Nd:YAG interferometry results. For a rod, the y direction is defined as the direction parallel to the polarization of the probe beam. In the y direction, the focal power of the slab and rod were -0.13 diopters and 2.71 diopters respectively. In the x direction the values were -0.47 diopters and 2.31 diopters. The difference in focal lengths is also less for the slab, at -0.29 diopters as compared to 0.40 diopters for the rod. The focal lengths of the rod for the two directions differ because the thermal stress creates birefringence. The ratio of focal lengths has been calculated for a uniformly pumped rod by Koechner [3]. Our observed ratio of 1.17 is close to his theoretical value of 1.2. The thermal effects in the slab are well described by an elliptical lens, as is shown by the fact that the root-mean-square deviation from a ellipsoidal surface is no more than one-tenth wave at 633 nanometers.

The output power of the laser was measured as a function of the lamp power for both the YAG slab and rod and for both multimode and TEM₀₀ operation. In all cases the output coupler was a 10% transmitting mirror. The parameters of a linear least square fit gave the threshold and the slope

efficiency for each case. Table 3 lists these values, as well as the output power achieved at the maximum lamp input power of 5.1 kilowatts. The multi-mode slab power was corrected to take into account the fact that the beam was filling only 69% of the pumped volume. This correction was used only for multimode operation and is discussed more fully later. The slab was nearly as efficient as the rod it replaced. The slope efficiencies for slab and rod were 2.25% and 2.36% respectively for multimode operation. For TEM₀₀ operation the values were 0.47% and 0.51%. The extrapolated threshold for the rod was about 10% more than that of the slab, in both cases. This is probably the result of the fact that the zigzag geometry results in the path through the slab being 15% longer than the path through the rod, with the gain correspondingly increased.

ORIGINAL PAGE IS
OF POOR QUALITY

A key factor in the efficiency of a laser is the geometric filling factor, given by the ratio of the volume effectively swept by the laser beam to the total pumped volume. When total laser power is the only concern, a multimode beam may be used, which expands to fill any aperture. Under these conditions the rectangular aperture is not a disadvantage. The 69% filling factor used for correcting multimode data was the result of the restricting aperture of the slab holder. The pump cavity was designed for rod use and it was not possible to access the full rectangular aperture of the slab without extensive modifications. No filling factors were used to correct data for TEM₀₀ operation. The portion of the slab blocked by the holder was outside the Gaussian beam. Similar efficiencies were observed even though the slab with 2:1 rectangular cross-section had a smaller filling factor than the rod. This is a result of reduced birefringence in the slab. The complex pattern of birefringence in the rod made necessary a smaller aperture to restrict oscillation to the TEM₀₀ mode.

Slabs with an aspect ratio of two have been used because we initially

believed that depolarization and non-elliptical focussing would be severe near the edge of the slab, and that the edge region was not useful. This was not observed to be the case. The measurements of depolarization and residual distortion described above, as well as recent theoretical work, show that it is possible to use the entire slab aperture. In the future we will be reporting on theory and measurements using slabs with an aspect ratio of one.

ORIGINAL PAGE IS
OF POOR QUALITY

The birefringence of the pumped slab and rod was found by measuring the transmittance of 633-nanometer light through crossed polarizers with the pumped slab or rod between the polarizers. Table 1 describes the depolarization of the GGG slab in each of its configurations, and Table 2 includes data for the Nd:YAG slab and rod. The GGG data show that depolarization in the slab was reduced from 4.5% to 0.2% when insulation and shielding were added. At all pump powers greater than 2 kilowatts, close to 25% of the 633-nanometer light passing through the YAG rod changed polarization. The corresponding value for the YAG slab, with shields and insulation, was 0.2% at 4.2 kilowatts of lamp power.

The degree of polarization of the Nd:YAG slab laser output was measured for both multi-mode and single transverse mode operation. We used an analyzer with an extinction ratio of 1000 to 1 and observed only single polarization output up to the maximum pump power of 5.1 kilowatts. It was not possible to control the polarization of the rod. In the multimode rod case, power was present equally in both polarizations. The single mode rod output was 90% in one polarization, but an attempt to control the direction of the polarization with a Brewster plate reduced the power drastically.

The same compensation that reduces depolarization due to thermal stress in slabs also reduces depolarization in slabs cut from highly stressed crystals

of Nd:YAG. Often crystals of Nd:YAG show unacceptable birefringence even when not pumped, due to stress in the crystal that results from the growth process. We obtained two Nd:YAG rods that showed depolarization in stressed regions of 17% and 10% respectively, for light of wavelength 633 nanometers. These rods were first cut into a slabs with a simple straight-through path. Depolarization was reduced very slightly, to 14% and 9%. When the ends were cut to allow a zig-zag path with 7 internal reflections, the depolarization of each was 0.3% or less, for light polarized along the axes of the slab.

We conclude that the zigzag slab laser geometry has very significant advantages which are easily available after small modifications to an existing Nd:YAG laser system. The only disadvantage is a small increase in cost due to the more difficult fabrication of the slab and the greater amount of Nd:YAG which is needed to allow the ends to be unpumped. We predict that YAG slabs will show similarly reduced thermal focussing and birefringence up to the fracture limit of the material. The fracture limit of a Nd:YAG slab or rod is near 500 Watts of output power from a 15 centimeter long crystal.

ORIGINAL PAGE IS
OF POOR QUALITY

ACKNOWLEDGMENTS

The authors thank Frank Bruni of the Materials Progress Corporation for providing the Nd:GGG crystal. This work was supported by the U. S. Army under grant #DAAG29-81-C-0038 and NASA under grant #NAG1-182.

REFERENCES

- [1] L. M. Osterink and J. D. Foster, "Thermal effects and transverse mode control in a Nd:YAG laser," Appl. Phys. Lett., vol. 12, pp. 128-131, 1968.
- [2] J. D. Foster and L. M. Osterink, "Thermal effects in a Nd:YAG

laser," J. Appl. Phys., vol. 41, pp. 3656-3663, 1970.

ORIGINAL PA
OF POOR QU

[3] W. Koechner, "Thermal lensing in a Nd:YAG laser rod," Appl. Opt., vol. 9, pp. 2548-2553, 1970.

[4] W. Koechner, Solid State Laser Engineering. New York: Springer, 1976, ch. 7.

[5] W. S. Martin and J. P. Chernoch, "Multiple internal reflection face pumped laser," U. S. Patent 3,533,126, 1972.

[6] W. B. Jones, L. M. Goldman, and J. C. Almasi, "Performance characteristics of two face pumped face cooled glass laser," Techn. Rep. AFAL-TR-72-233, General Electric Research and Development, Schenectady, N.Y., 1972.

[7] G. J. Hulme, W. B. Jones, "Total internal reflection face pumped laser," Proc. Soc. Photo-Optical Instr. Eng., 69, pp. 38-45 (1975).

[8] J. M. Eggleston, T. J. Kane, J. Unternahrer, and R. L. Byer, "Slab-geometry Nd:glass laser performance studies," Opt. Lett., vol. 7, pp. 405-407, 1982.

[9] J. M. Eggleston, "Theoretical and experimental studies of slab geometry lasers," Ph. D. dissertation. Stanford University, 1982.

[10] "Selection guide to electrical/electronic materials from Dow Corning." Dow Corning Corporation, Midland, Michigan.

Captions

Fig 1. (a) The zigzag slab laser geometry, with shields and insulation.
(b) Ray path through the zigzag slab. Note that slabs with an odd number of

total internal reflections are possible, and in that case the end faces are not parallel.

Fig. 2. Interferograms of the Nd:GGG slab pumped at 4.2 kilowatts cw power, showing the importance of end and edge effects. (a) No edge insulation, no end shields. (b) Edge insulation, but no end shields. (c) End shields, but no edge insulation. (d) Edge insulation and end shields.

Fig. 3. Interferograms of Nd:YAG rod and slab pumped at 4.2 kilowatts cw show substantial advantages of zigzag slab geometry.

ORIGINAL PAGE IS
OF POOR QUALITY

TABLE I

Effects of Shields and Insulation on Focal Power
and Depolarization for Nd:GGG Slab at 4.2 Kilowatts

Shields		No	Yes	No	Yes
Insulation		No	Yes	No	Yes
Focal Power (Diopters)	X	1.35	1.05	-0.54	-0.25
	Y	-2.34	-0.40	-2.82	-0.46
Depolarization (percent)		4.5	0.5	1.5	0.2

TABLE II

Focal Power, Distortion and Depolarization
for Nd:YAG Slab and Rod at 4.2 kW

	Direction	Slab	Rod
Focal Power (Diopters)	X	-0.47	2.31
	Y	-0.18	2.71
Residual Distortion (HeNe Wavelengths)	X	0.03	0.16
	Y	0.10	0.36
Depolarization (percent)		0.2	25.0

TABLE III

Threshold, Slope Efficiency and
Power for Nd:YAG Slab and Rod

		Threshold (kilowatts)	Slope Efficiency (percent)	Output, lamp at 5.1 kilowatts (Watts)
Multimode	Slab	1.55	2.25	83
	Rod	1.70	2.36	88
TEM ₀₀	Slab	2.03	0.47	13.0
	Rod	2.25	0.51	13.8



4946-1

ORIGINAL PAGE IS
OF POOR QUALITY

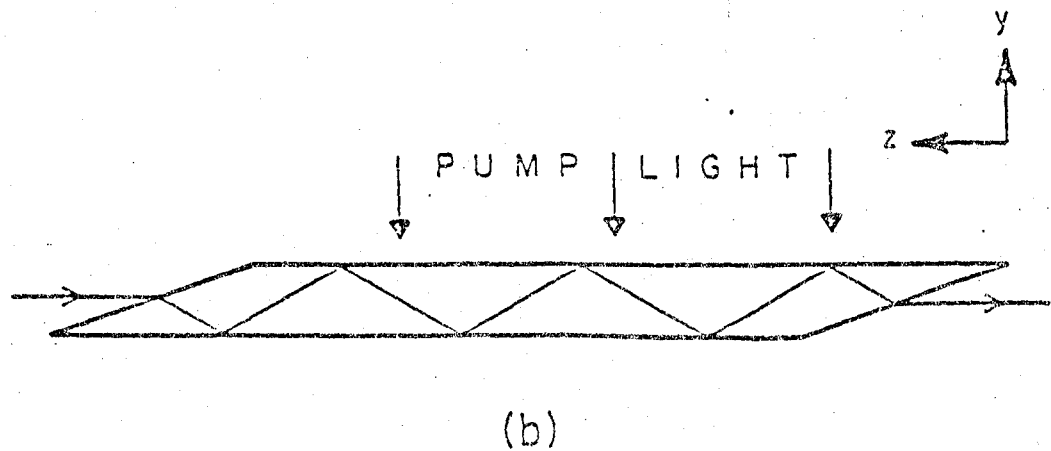
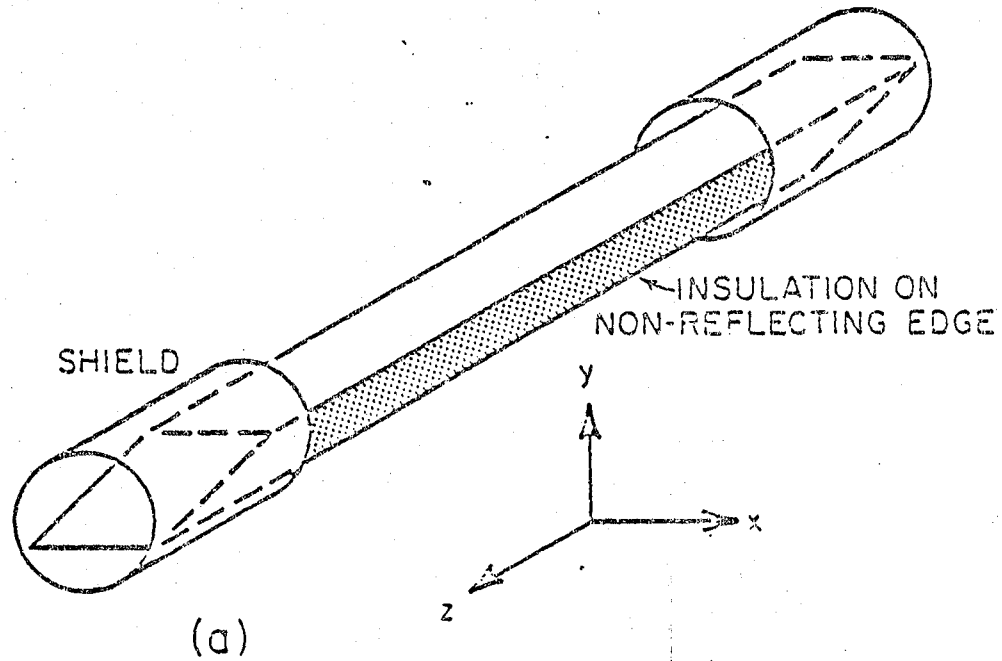
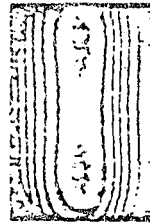


FIGURE 1

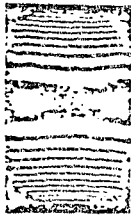
ORIGINAL PAGE IS
OF POOR QUALITY



(a)



(b)



(c)



(d)

FIGURE 2



ORIGINAL PAGE IS
OF POOR QUALITY

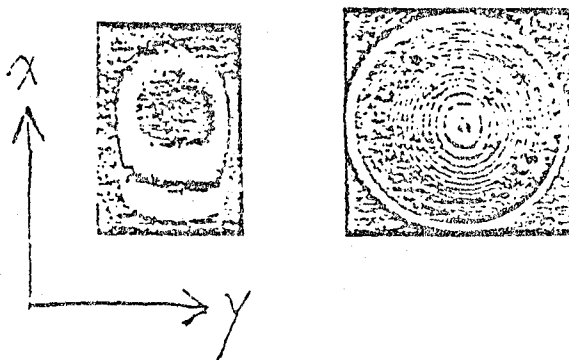


FIGURE 3

End of Document